Tetrahedron 65 (2009) 9801–9806

Contents lists available at ScienceDirect

Tetrahedron

journal homepage: www.elsevier.com/locate/tet

Characterization of low molecular-weight gelator methyl-4,6-*O*-(*p*-nitrobenzylidene)-α-D-glucopyranoside hydrogels and water diffusion in their networks

Joanna Kowalczuk [a], Sławomir Jarosz [b], Jadwiga Tritt-Goc [a,*]

[a] *Institute of Molecular Physics, Polish Academy of Sciences, ul. M. Smoluchowskiego 17, 60-179 Poznań, Poland*
[b] *Institute of Organic Chemistry, Polish Academy of Sciences, ul. Kasprzaka 44/52, 01-224 Warszawa, Poland*

ARTICLE INFO

Article history:
Received 19 August 2009
Accepted 17 September 2009
Available online 19 September 2009

Keywords:
Sugar-based organogelator
Hydrogel
Gel–sol transition
Water dynamics
Diffusion
Spin-lattice relaxation

ABSTRACT

This paper focuses on the thermal properties, the microstructure, and the molecular dynamics of water in the hydrogels (1.5, 2, 3, 4, and 5% [g mL^{-1}]) formed by sugar-based low molecular-weight gelator methyl-4,6-*O*-(*p*-nitrobenzylidene)-α-D-glucopyranoside. The energy needed to break the non-covalent interactions such as the hydrophobic, dipole–dipole, and π–π stacking interactions responsible for the gel formation was calculated to be 43 kJ mol^{-1}. The microstructure of the 4% [g mL^{-1}] hydrogel shows a characteristic fibril structure of the gel network with individual gel fibers, the junction points of thicker fibers, and pores occupied by water. The single mode diffusion of water molecules inside the gel network was detected irrespective of the diffusion time Δ (8–75 ms) and hydrogel concentration. For Δ of 10 ms the water diffusion is almost free and characterized by the diffusion coefficient in the range from 2.17×10^{-9} to 1.84×10^{-9} m^2 s^{-1} for studied hydrogels. For larger Δ values, so-called restricted diffusions are observed and manifested in the linear decreases of the diffusion coefficient with diffusing time Δ, as shown for 5% gel. Only the one average proton spin-lattice relaxation time T_1 of water was determined for the studied hydrogels, irrespective of gelator concentration.

1. Introduction

Organogels are a new class of nanostructured materials, which are composed of a self-assembled superstructure of low molecular-weight gelators (LMWGs) and a large volume of organic solvent immobilized therein. The driving forces for molecular aggregation are non-covalent interactions such as dipole–dipole, van der Waals, π–π stacking or hydrogen-bonding interactions.[1–6] There is a tendency to classify the gelators according to their driving force for molecular aggregation into two categories: non-hydrogen-bond-based[7] and hydrogen-bond-based gelators.[8–20] However, this classification is very general because in many cases the aggregation of the gelator molecules into fibrous networks takes place through a combination of interactions.[1,21,22] In recent years, organogels were the subject of great interest and many studies due to their numerous industrial applications and interesting supramolecular structures.[1–5]

There are many different types of gelators and their corresponding gels, and among them of special interest are sugar-based organogels.[17–27] They form a large library of compounds with potential use as building blocks for new gelators with different gelation abilities and different three-dimensional network structures. However, discovery of a good gelator is very often the matter of chance. On the other hand, the careful studies of such a large group of similar compounds can help to predict the conditions, which molecules have to fulfill to be a good gelator. In recent years, sugar-based organogels were widely explored and we learned that they have high potential in gel formation, but some of them do not form gels at all. The main driving forces for molecule aggregation in organogels are hydrogen-bond interactions. It was proven by FTIR and NMR spectroscopy that directional hydrogen-bond networks in a single crystal of saccharide-containing gelators is a basic requirement for a saccharide to be a good gelator.[19,20,24] Sugar-based gelators possess the ability to gelatinize a wide spectrum of solvents but they do not generally make gels with water. Mostly, hydrogels are made of polymer molecules through complicated intermolecular interactions. There are relatively few examples of hydrogels composed of LMWGs[3,15,16,28–32] and particularly of sugar-based gelators.[33–37] The cause is that water can act as a hydrogen-bond acceptor and weakens any network formation based on intermolecular hydrogen-bonding interactions or increases the dimensionality, thus making the gelation process difficult.

The subject of our studies is methyl-4,6-*O*-(*p*-nitrobenzylidene)-α-D-glucopyranoside (**1**) with a chemical structure presented in Figure 1. It is a unique sugar-based gelator, which has gelation ability

* Corresponding author. Tel.: +48 061 8695 226.
E-mail address: jtg@ifmpan.poznan.pl (J. Tritt-Goc).

0040-4020/$ – see front matter © 2009 Elsevier Ltd. All rights reserved.
doi:10.1016/j.tet.2009.09.073

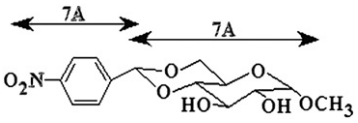

Figure 1. Chemical structure of 4,6-*O*-(*p*-nitrobenzylidene)-α-D-glucopyranoside.

in organic solvents as well as in water. Examples of such 'bifunctional' gelators are limited in the literature.[21] The crystal structure for compound **1** has not been examined but the structure is known for the unsubstituted gelator, i.e., methyl-4,6-*O*-benzylidene-α-D-glucopyranoside.[18,23] This compound has two unmodified hydroxyl groups, 2-OH and 3-OH, one hydroxyl group protected by a methyl group 1-OH, and 4-OH and 6-OH groups protected by a benzylidene group. In the crystal state, the unsubstituted gelator forms one-dimensional zigzag chains in which molecules are connected by two intermolecular hydrogen bonds using the hydroxyl group's 2-OH and 3-OH. The studied gelator **1** differs only by the nitro group attached to the benzylidene in the *para*-positon (Fig. 1). Therefore, we can assume that the crystal structure of gelator **1** is very similar to the unsubstituted one.[18,23] The introduction of the *p*-nitro-substituent only in *para*-positon increases the tendency for self-aggregation of methyl-4,6-*O*-benzylidene-monosaccharides.[25]

In nonpolar solvents the hydrogen-bond interactions are the driving forces for self-assembly of this type of gelators, whereas in water, other aggregation modes such as dipole–dipole, hydrophobic or π–π stacking interactions dominate self-assembly.[21,25] This gelator has been used for the preparation of a novel donor–acceptor, sugar-based gelator system serving as an acceptor group. This type of a dual component organogel exhibits a charge transfer interaction.[22,37]

The unique properties of gelator **1** were the inspiration of our studies presented in this paper. We focus in this discussion on the thermal properties, the microstructure of **1** hydrogel, and on the molecular dynamics of water in the gel network structure. This is an important topic given that many researchers are interested in exploiting the dynamics environment inside hydrogels for a range of applications, such as tissues engineering.[38]

2. Results and discussions

2.1. Gel–sol phase transition

Thermally reversible gel-to-sol phase transitions are a characteristic feature of hydrogels formed by **1** because the physical gelation of **1** occurs via self-aggregation through non-covalent interactions. Figure 2 shows the influence of gelator concentration on the thermal properties of the studied hydrogels. The T_{gs} and thus

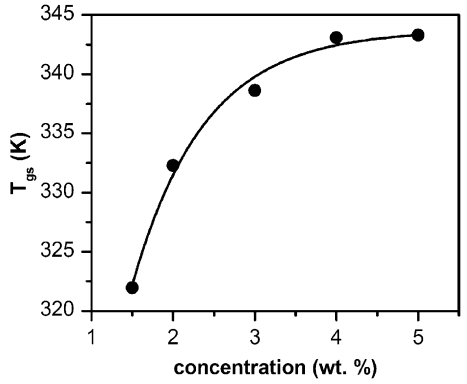

Figure 2. Dependence of T_{gs} on the concentration of 4,6-*O*-(*p*-nitrobenzylidene)-α-D-glucopyranoside hydrogel. The solid line has no physical meaning and is included as a visual guide.

the thermal stability of hydrogel exponentially increase with the increase of the gelator concentration up to 4% [g mL^{-1}]. Above this concentration no dependence of the phase transition on concentration was observed.

It is accepted that the gel-to-sol phase transition can be considered as a dissolution process of microcrystals and is described by Eq. 1 derived from Schrader's relation[39]

$$\log[C] = -\frac{\Delta H}{2.303R} \times \frac{1}{T_{gs}} + constant \quad (1)$$

where C is the molar gel concentration, ΔH is the melting enthalpy, R is the gas constant and T_{gs} the gel-to-sol transition temperature.

Eq. 1 was originally proposed for the gel–sol phase transition for polymeric networks whose crosslink formation is made up of pairs of chains and does not take into account the influence of the solvent, which may affect the structures and thermodynamic behaviors.[40] Thus, using it for describing the physical gel is probably oversimplified but is generally accepted.

In the case of the studied hydrogels the use of the Eq. 1 to analyze the dependence of the gel-to-sol phase transitions is justify because the small-angle X-ray scattering (SAXS) measurements showed that the gel fiber composed of the aggregates of the **1** molecule in the gels made with the organic solvent are related to the crystal.[22] Thus, we can assume that also the hydrogel fibers of **1** poses a more or less crystal-like structure. Therefore, ΔH of **1** hydrogel was determined from the slope of log (concentration of gelator molecules) versus $1000/T_{gs}$—Figure 3. The best fit, with a correlation coefficient γ of 0.9589, is shown as the solid line in Figure 3 and the fitting parameter ΔH is equal to 43 kJ mol^{-1}. The obtained value correspond well with that reported up to now for the other monosaccharides-based gels where the energies were also determined with the help of Eq. 1.[19,20,24]

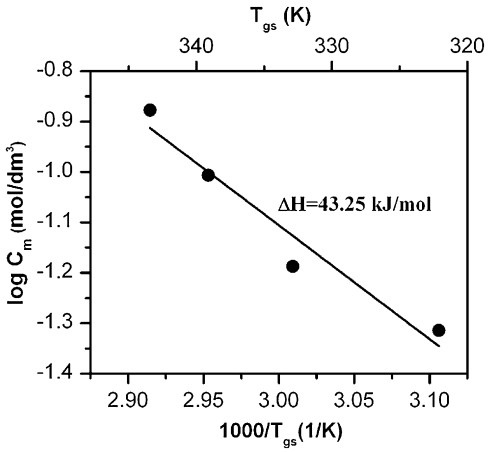

Figure 3. Plot of the logarithm of gelator concentration versus the reciprocal absolute temperature of T_{gs} The solid line is the best fit of Eq. 1 to the experimental points.

The gel–sol transition is a structural transition phenomenon related to the disruption of the non-covalent interactions within the gelator network. The question arises about the particular type of these interactions. The driving forces for self-assembly of methyl-4,6-*O*-benzylidene-monosaccharides and other sugar-based gelators in nonpolar solvents are hydrogen-bond interactions.[9–20,25] In polar solvents, other types of interactions should be considered, because in water or alcohols, solvent molecules can act as competing hydrogen-bond donors and acceptors and suppress the self-aggregation mechanism of gelator molecules

based on hydrogen-bonding interactions. ^{1}H NMR measurements showed that combined interactions can occur when the sugar-based gelators aggregate in water e.g., the intermolecular hydrogen-bonding and π–π stacking interactions.[21,11] However, the latter type of interaction between the *p*-nitrophenyl groups in the **1** hydrogel was not directly evidenced by CD and ^{1}H NMR spectroscopy.[25] Therefore, it was assumed that the hydrophobic and dipole–dipole interactions are the main aggregation modes for **1** in water.[25] The former interaction takes place between the gelator and water molecules whereas the latter one between the highly polarized nitro groups.

The π–π stacking interactions, despite no experimental evidence, should also play an important role in the fibrous aggregate formation in the studied hydrogel because in water the intermolecular hydrogen-bond interactions among the hydroxyl groups of gelator molecules are no longer strong enough to maintain the fibril structure.[25]

Therefore, it is reasonable to assume that combined non-covalent interactions such as the hydrophobic, dipole–dipole, and π–π stacking interactions are the driving forces for molecular aggregation of **1** in water. If so, we conclude that the calculated value of ΔH=43 kJ mol^{-1} is the energy needed to break these interactions and dissolve the gelator aggregates.

For the studied hydrogels, the phase transition (the dissolution of all the gel) occurs over a broad temperature range of about ΔT=18 K indicating the inhomogeneous microstructure of their networks. Otherwise, a narrow phase transition range of about 2–5 K is expected.

2.2. Optical polarization microscopy observation of hydrogel

The visual image of the microstructure of the gelator network of **1** in 4% hydrogel is presented in Figure 4. A characteristic fibril structure of the gel network is clearly visible despite the fact that the image was taken with the Optical Polarization Microscopy not with Scanning Electron Microscopy spectrometer. The well resolved images taken by OPM method were also obtained for other sugar-based gels.[20,41] The image in Figure 4 showed that the individual gel fibers bundled together to make thicker fibers, which in turn can cross and stick together to make the junction points. The water in the hydrogel occupies the blank regions often called pores, spaces, pools or compartments.

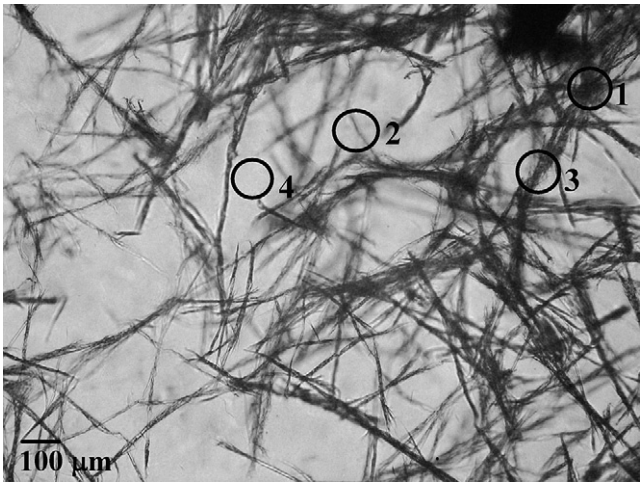

Figure 4. Optical polarization microscopy image of hydrogel at 4% (g mL^{-1}) concentration of gelator **1**. The junction points (1), the individual gel fibers (2), the bundle of the gel fibers (3) together with the blank regions occupied by the water (4) are visible.

2.3. Diffusion behavior of water molecules in the hydrogel network

PGSE ^{1}H NMR is a very important method in measuring the self-diffusion coefficient of small molecules in the presence of the gelator network[42–44] and therefore was employed to obtain the diffusion behavior of water in the hydrogel matrix formed by **1**. The experimental results of the echo decay amplitude for water molecules in 1.5, 3, and 4% [g mL^{-1}] hydrogels, respectively are presented in Figure 5. Values were obtained by varying field gradient strength *g*, with the constant diffusion time Δ=10 ms, and at 27 °C. The data lie on the straight lines indicating single mode diffusion. Therefore, the single diffusion coefficients were determined from the slope of the corresponding lines by Eq. 2.

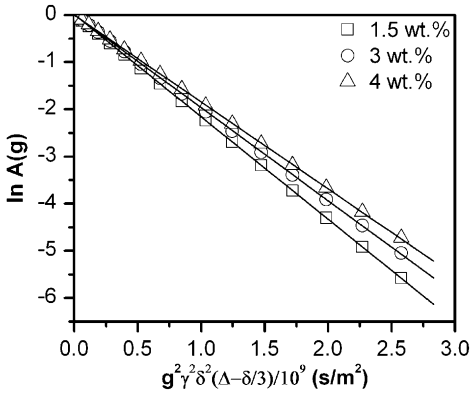

Figure 5. Diffusion echo attenuation of water molecules in **1** hydrogels of different concentration. Values were obtained by varying field gradient strength *g*, with the diffusion time Δ=10 ms, and at 27 °C.

The diffusion coefficients are plotted in Figure 6 and as can be seen decrease with the increase of gelator concentration (the decrease of water content).

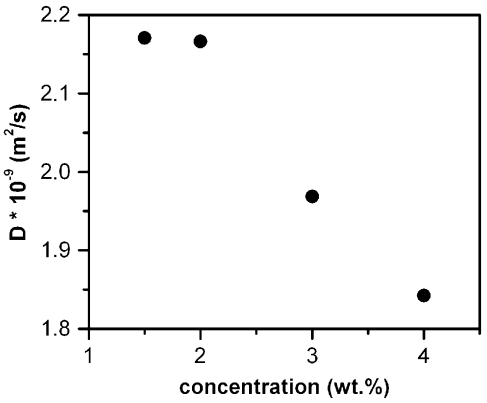

Figure 6. Diffusion coefficient *D* of water molecules in **1** hydrogels as a function of gelator concentration.

For 5% hydrogel of **1** the diffusion measurements were performed with varying Δ in the range from 8 to 75 ms. The amplitudes of the echo attenuation lie on the straight lines in this Δ delta range but the slope of the plots are dependent of the diffusion time. The calculated diffusion coefficients linearly decrease as a function of Δ (Fig. 7).

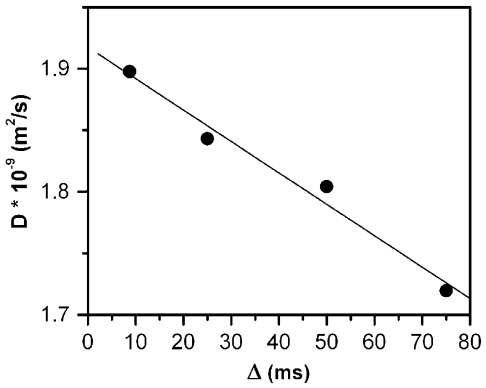

Figure 7. Dependence of diffusion coefficient D of water molecules in hydrogel at 5% ($g\,mL^{-1}$) concentration of gelator **1** on the diffusion time Δ.

The hydrogels made by the LMOGs consist of a very large amount of water confined within the gel network composed from the entangled fibrils formed by the gelator aggregates. Thus, the gel network can be treated as a macroscopically porous matrix with pores (often called spaces, pools or compartments) of different sizes and shapes (see, for example, Fig. 4). The water motion is arresting on the macroscale but has the ability to diffuse inside the pores.

In the PGSE NMR experiment, we measure the echo signal, that is, the sum of the signals corresponding to water molecules within the different pores. The measured diffusion coefficient D is an average value of the different diffusion constant characterized the motion of the water in different compartments.

The diffusion coefficients for the measured hydrogels of **1** (Fig. 6) are of the same order as for bulk water at 27 °C ($2.30\times10^{-9}\ m^2\,s^{-1}$) indicating almost free diffusion at least in the time scale of the measurements. The linear dependence ($\gamma=1$) of the echo attenuation vs gradient strengths (Fig. 5) obtained during the diffusion measurements also allows us to discard the presence of barriers to the translational motion of water during the diffusion time $\Delta=10$ ms.

By substituting the calculated D values of water in hydrogels of **1** (2.17×10^{-9}, 1.97×10^{-9}, and $1.84\times10^{-9}\ m^2\,s^{-1}$) into Eq. 5, the diffusion distances are calculated to be 6.3, 6.0, and 5.8 μm for 2, 3, and 4% hydrogels, respectively. Thus, on average, the size of the pores in which the water molecules are confined in particular hydrogels must be larger than these diffusion distances because free diffusion is observed. The results are consistent with the network structure shown for 4% hydrogel in Figure 4. We can conclude that for a diffusion time of 10 ms the water molecules are not able to reflect the network structure. The pores are sufficiently large and thus the gel matrix does not affect or obstruct the motion of the water molecules. The observed decrease of the diffusion coefficient observed as a function of gelator concentration is the result of the slightly dense structure of the gelator matrix.

When increasing the diffusion time, the sizes of the compartments in this gel matrix filled with water may become comparable with the diffusion distance of water and the confinement effect starts to play a role. As a result, so-called restricted diffusion[45] is observed and manifested in the linear decreases of the diffusion coefficient with diffusing time Δ as observed for 5% hydrogel of **1** ($\gamma=0.9999$)—Figure 7. Therefore, for the same size of the solvent molecule (the water molecule) and the same structure of the gel matrix (5% gel of **1**), by changing the diffusion time even in the narrow range from 8 to 75 ms we are able to detect the heterogeneity of matrix.

2.4. Spin-lattice measurements of water in the hydrogel network

We can assume that the pores within the studied hydrogel matrix are hydrophilic because of the hydroxyl groups of which the gelator molecules of **1** are composed. The water molecules can interact with the surface of the network. If so, at least two types of water can be distinguished in the gels: bound water, strongly associated with the gelators molecules by the hydrogen bonds and the bulk water whose properties are not affected by the presence of gel network.[46] The proton spin-lattice relaxation T_1 measurements can distinguish these types of water. However, this is not the case for the studied hydrogels. In our experiment, the monoexponential recoveries of magnetization were measured and thus only one T_1 was determined for particular hydrogels of **1**. The T_1 data as a function of gelator concentration are shown in Figure 8.

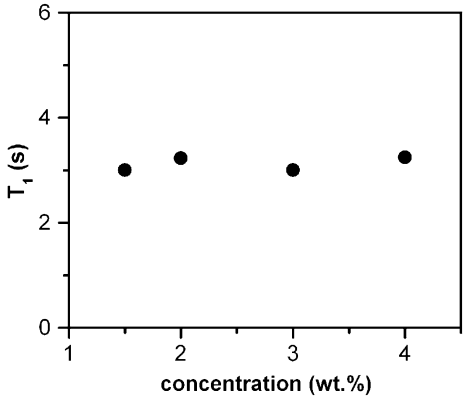

Figure 8. Proton spin-lattice relaxation time of water molecules in **1** hydrogels as a function of gelator concentration at 27 °C.

The relaxation measurements were performed at 27 °C and at this temperature it is reasonable to assume that the water molecules are in fast diffusive exchange with respect to the spin-lattice relaxation time. Consequently, only one average spin-lattice relaxation time is measured. The T_1 data are irrespective of gelator concentration.

3. Conclusion

In this paper we measured the thermal properties of hydrogel formed by sugar-based low molecular-weight gelator methyl-4,6-*O*-(*p*-nitrobenzylidene)-α-D-glucopyranoside. The determined value of the gel–sol transition enthalpy (43 $kJ\,mol^{-1}$) corresponds well with the values reported for the other monosaccharides-based gels.[19,20,24] The gelator **1** forms in water a characteristic fibril structure of the gel network with individual gel fibers, the junction points of thicker fibers, and pores occupied by water. Using water as a probe molecule and the same structure of the gel matrix (5% gel of **1**), by changing the diffusion we are able to detect the heterogeneity of hydrogel matrix.

4. Experimental

4.1. Preparation of 4,6-*O*-(*p*-nitrobenzylidene)-α-D-glucopyranoside (1) and its hydrogels

Compound **1** was synthesized according to the method described elsewhere.[25] Concentrations of 1.5 2, 3, 4, and 5% [$g\,mL^{-1}$] of **1** were chosen to form the gels with water. The gels are prepared by mixing the appropriate amount of the gelator and water in a closed capped tube and heating the mixture until the solid was dissolved. Cooling the solution below the characteristic gelation temperature T_{gs} causes the transition to the gel phase. As a result thermoreversible, slightly opaque gels were obtained for each concentration.

4.2. Microscopic observation

Optical Polarization Microscopy investigation (OPM) was performed with a JENAPOL microscope operating in different contrast and polarization mode. A drop of 4% [g mL^{-1}] of **1** hydrogel was carefully cast onto glass microscope slides and immediately was subjected to OPM observation.

4.3. Gel–sol phase transition measurements

Transition temperatures of hydrogels formed by **1** were determined using the air-bath method and visual inspection of the samples. The air-bath method involves inserting a sealed glass vial with the gel sample into a stream of air whose temperature changes are precisely controlled. For this purpose we used the NMR probe head with standard temperature control system. Visual inspection of the sample was possible due to a slight modification of the probe head. The opaque RF coil was replaced by a transparent glass tube. The temperature of the gel–sol (T_{gs}) transition was determined upon heating the sample to the temperature at which the system starts to flow. The temperature of the sample was measured with an accuracy of ±0.1 °C.

4.4. Diffusion and spin-lattice relaxation measurement

Diffusion coefficient (D) and ^{1}H spin-lattice relaxation (T_1) measurements of water in the hydrogels network were carried out on a Bruker AVANCE pulse spectrometer operating at 300 MHz spectrometer equipped with magnetic field gradients. The diffusion coefficients were calculated using the pulse gradient spin echo (PGSE) pulse sequence introduced by Stejskal and Tanner.[47] The D values were determined by using the relationship between the echo signal intensities and field gradient parameter:

$$A(g) = A(0)\exp\left[-\gamma^2 g^2 D\delta^2\left(\Delta-\frac{\delta}{3}\right)\right] \quad (2)$$

where $A(g)$ and $A(0)$ are echo signal intensities at $t=2\tau$ with and without the field gradient pulse being the strength g, respectively. τ is the pulse interval, γ the magnetogyric ratio of the proton, g is the field gradient strength, δ the duration of the gradient pulses, and Δ is the gradient pulse interval, which is called the diffusing time. The echo signal intensity was measured as a function of g and the plot of ln $A(g)$ against $\gamma^2 g^2 \delta^2(\Delta-\delta/3)$, so-called Stejskal–Tanner plot, gives a straight line with a slope of $-D$ if the studied sample consists of a single component. This means that the D value can be determined from its slope by fitting Eq. 2 to the experimental points.

If the diffusion of the sample consists of multicomponents, at least in the measurement time scale, the total echo attenuation is given by a superposition of contribution from the individual components.

$$A(g) = A(0)\sum f_i \exp\left[-\gamma^2 g^2 D_i \delta^2\left(\Delta-\frac{\delta}{3}\right)\right] \quad (3)$$

were f_i and D_i are the fractional proton number and diffusion coefficient of the ith component, respectively.

The field gradient strength g values employed in our experiment are 0–1000 mTm^{-1}, in equal intervals of 60 mTm^{-1}. The diffusion coefficients D in the function of gelator concentration were studied for the gradient pulse interval Δ equal 10 ms whereas for 5% [g mL^{-1}] gel for the Δ values equal 8.7, 25, 50, and 75 ms, respectively. The duration of the gradient δ in all experiments was 2 ms. The measurements were performed along the z direction of the cylindrical gel sample and at 27 °C.

The diffusion coefficient D can be related with mean-square displacement $\langle\Delta z\rangle^2$ in the z direction from the starting point after the diffusion time Δ by the following equation:

$$\langle z^2\rangle = 2Dt \quad (4)$$

where t is equal to $\Delta-\delta/3$. The diffusion distance d measured in the experiment can be expressed by the following equation:

$$d = \sqrt{2Dt} \quad (5)$$

Proton spin-lattice relaxation time T_1 was determined by inverse recovery method using an 180°-τ-90° pulse sequence. The τ value denoted the variable delay time. The recovery of the magnetization was found to be exponential within experimental error at all concentrations of gelator **1**. The relaxation measurements were carried out at 27 °C and the errors in the measurements were estimated to be about 3–5%.

Acknowledgements

This work has been supported by funds for sciences in years 2007–2009 as research project N N202 1441 33.

References and notes

1. Weiss, R. G.; Terech, P. *Molecular Gels, Materials with Self-assembled Fibrillar Network*; Springer: Dordrecht, The Netherlands, 2006.
2. George, M.; Weiss, R. G. *Acc. Chem. Res.* **2006**, *39*, 489–497.
3. Estroff, L. A.; Hamilton, D. *Chem. Rev.* **2004**, *104*, 1201–1218.
4. Terech, P.; Weiss, R. G. *Chem. Rev.* **1997**, *97*, 3133–3159.
5. Llusar, M.; Sanchez, C. *Chem. Mater.* **2008**, *20*, 782–820.
6. Terech, P.; Furman, I.; Weiss, R. G. *J. Phys. Chem.* **1995**, *99*, 9558–9566.
7. Murata, K.; Aoki, M.; Suzuki, T.; Hanada, T.; Kawabata, H.; Komori, T.; Oseto, F.; Ueda, K.; Shinkai, S. *J. Am. Chem. Soc.* **1994**, *116*, 6664–6676.
8. James, T. D.; Murata, K.; Harada, T.; Ueda, K.; Shinkai, S. *Chem. Lett.* **1994**, 273–276.
9. Hanabusa, K.; Okui, K.; Karaki, K.; Shirai, H. *J. Chem. Soc., Chem. Commun.* **1992**, 1371–1374.
10. Hanabusa, K.; Yamada, Y.; Kimura, M.; Shirai, H. *Angew. Chem., Int. Ed.* **1996**, *35*, 1949–1951.
11. Hanabusa, K.; Shimura, K.; Hirose, K.; Kimura, M.; Shirai, H. *Chem. Lett.* **1996**, 885–886.
12. Hanabusa, K.; Kawakami, A.; Kimura, M.; Shirai, H. *Chem. Lett.* **1997**, 191–192.
13. de Vries, E. J.; Kellogg, R. M. *J. Chem. Soc., Chem. Commun.* **1993**, 238–240.
14. Takafujii, M.; Ihara, H.; Hirayama, C.; Hachisoko, H.; Yamada, K. *Liq. Cryst.* **1995**, *18*, 97–100.
15. Yoza, K.; Ono, Y.; Yoshihara, K.; Akao, T.; Shinmori, H.; Takeuchi, M.; Shinkai, S.; Reinhoudt, D. N. *Chem. Commun.* **1998**, 907–908.
16. Yoza, K.; Amanokura, N.; Ono, Y.; Akao, T.; Shinmori, H.; Takeuchi, M.; Shinkai, S.; Reinhoudt, D. N. *Chem.— Eur. J.* **1999**, *5*, 2722–2729.
17. Luboradzki, R.; Gronwald, O.; Ikeda, M.; Shinkai, S.; Reinhoudt, D. N. *Chem. Lett.* **2000**, 1148–1149.
18. Luboradzki, R.; Gronwald, O.; Ikeda, M.; Shinkai, S.; Reinhoudt, D. N. *Tetrahedron* **2000**, *56*, 9595–9599.
19. Tritt-Goc, J.; Bielejewski, M.; Luboradzki, R.; Łapiński, A. *Langmuir* **2008**, *24*, 534–540.
20. Bielejewski, M.; Łapiński, A.; Kaszyńska, J.; Luboradzki, R.; Tritt-Goc, J. *Tetrahedron Lett.* **2008**, *49*, 6685–6689.
21. Jung, J. H.; John, G.; Masuda, M.; Yoshida, K.; Shinkai, S.; Shimizu, T. *Langmuir* **2001**, *17*, 7229–7232.
22. Jeong, Y.; Friggeri, A.; Akiba, I.; Masunaga, H.; Sakurai, K.; Sakurai, S.; Okamoto, S.; Inoue, K.; Shinkai, S. *J. Colloid Interface Sci.* **2005**, *283*, 113–122.
23. Gronwald, O.; Shinkai, S. *Chem.— Eur. J.* **2001**, *7*, 4328–4334.
24. Gronwald, O.; Sakurai, K.; Luboradzki, R.; Kimura, T.; Shinkai, S. *Carbohydr. Res.* **2001**, *331*, 307–318.
25. Gronwald, O.; Shinkai, S. *J. Chem. Soc., Perkin Trans. 2* **2001**, 1933–1937.
26. Luboradzki, R.; Pakulski, Z.; Sartowska, B. *Tetrahedron* **2005**, *61*, 10122–10128.
27. Roy, S.; Chakraborty, A.; Ghosh, R. *Carbohydr. Res.* **2008**, *343*, 2523–2529.
28. Fuhrhop, J. H.; Schnieder, P.; Rosenbery, J.; Boekema, E. *J. Am. Chem. Soc.* **1987**, *109*, 3387–3390.
29. Fuhrhop, J. H.; Boettcher, C. *J. Am. Chem. Soc.* **1990**, *112*, 1768–1776.
30. Menger, F.; Caran, K. *J. Am. Chem. Soc.* **2000**, *122*, 11679–11691.
31. Hanabusa, K.; Hirata, T.; Inoue, D.; Kimura, M.; Touhara, H.; Shirai, H. *Colloids Surf., A* **2000**, *169*, 307–316.
32. Oda, R.; Huc, I.; Candau, S. J. *Angew. Chem., Int. Ed.* **1998**, *37*, 2689–2691.
33. John, G.; Masuda, M.; Okada, Y.; Yase, K.; Shimizu, T. *Adv. Mater.* **2001**, *13*, 715–718.

34. Masuda, M.; Hanada, T.; Okada, Y.; Yase, K.; Shimizu, T. *Macromolecules* **2000**, *33*, 9233–9238.
35. Nakazawa, I.; Masuda, M.; Okada, Y.; Hanada, T.; Yase, K.; Asai, M.; Shimizu, T. *Langmuir* **1999**, *15*, 4757–4764.
36. Shimizu, T.; Masuda, M. *J. Am. Chem. Soc.* **1997**, *119*, 2812–2818.
37. Friggeri, A.; Gronwald, O.; van Bommel, K. J. C.; Shinkai, S.; Reinhoudt, D. N. *J. Am. Chem. Soc.* **2002**, *124*, 10754–10758.
38. Hirst, A. R.; Escuder, B.; Miravet, J. F.; David, K.; Smith, D. K. *Angew. Chem., Int. Ed.* **2008**, *47*, 8002–80018.
39. Murata, K.; Aoki, K.; Suzuki, T.; Hanada, T.; Kawabata, H.; Komori, T.; Oseto, F.; Ueda, K.; Shinkai, S. *J. Am. Chem. Soc.* **1994**, *116*, 6664–6674 and references cited therein.
40. Garner, C. M.; Terech, P.; Allegraud, J. J.; Mistrot, B.; Nguyen, P.; de Geyer, A.; Rivera, D. J. *Chem. Soc. Faraday Trans.* **1998**, *94*, 2173–2179.
41. Bielejewski, M.; Łapiński, A.; Luboradzki, R.; Tritt-Goc, J. *Langmuir* **2009**, *25*, 8274–8279.
42. Kamiguchi, K.; Kuroki, S.; Satoh, M.; Ando, I. *Macromolecules* **2009**, *42*, 231–235.
43. Kamiguchi, K.; Kuroki, S.; Satoh, M.; Ando, I. *Macromolecules* **2008**, *41*, 1318–1322.
44. Nyden, M.; Soderman, O.; Karlstrom, G. *Macromolecules* **1999**, *32*, 127–135.
45. Price, S. W. *Annu. Rep. NMR Spectrosc.* **1996**, *32*, 51–142.
46. Fyfe, C. A.; Blazek, A. *Macromolecules* **1997**, *30*, 6230–6237.
47. Stejskal, E. O.; Tanner, J. E. *J. Chem. Phys.* **1965**, *42*, 288–292.